

Tuning the conductance of Dirac fermions on the surface of a topological insulator

S. Mondal,¹ D. Sen,² K. Sengupta,¹ and R. Shankar³

¹Theoretical Physics Division, Indian Association for the Cultivation of Sciences, Kolkata 700 032, India

²Center for High Energy Physics, Indian Institute of Science, Bangalore 560 012, India

³The Institute of Mathematical Sciences, C.I.T. Campus, Chennai 600 113, India

(Dated: April 2, 2024)

We study the transport properties of the Dirac fermions with Fermi velocity v_F on the surface of a topological insulator across a ferromagnetic strip providing an exchange field J over a region of width d . We show that the conductance of such a junction changes from oscillatory to a monotonically decreasing function of d beyond a critical J . This leads to the possible realization of a magnetic switch using these junctions. We also study the conductance of these Dirac fermions across a potential barrier of width d and potential V_0 in the presence of such a ferromagnetic strip and show that beyond a critical J , the criteria of conductance maxima changes from $\mu = eV_0 d \sim v_F = n$ to $\mu = (n+1/2)$ for integer n . We point out that these novel phenomena have no analogs in graphene and suggest experiments which can probe them.

PACS numbers: 71.10.Pm, 73.20.-r

Topological insulators in both two- and three-dimensions (2D and 3D) have attracted a lot of theoretical and experimental attention in recent years [1, 2, 3, 4]. It has been shown in Ref. [4] that such 3D insulators can be completely characterized by four integers ν_0 and $\nu_{1,2,3}$. The former specifies the class of topological insulators to be strong ($\nu_0 = 1$) or weak ($\nu_0 = 0$), while the latter integers characterize the time-reversal invariant momenta of the system given by $\mathbf{M}_0 = (\nu_1 \tilde{\mathbf{b}}_1; \nu_2 \tilde{\mathbf{b}}_2; \nu_3 \tilde{\mathbf{b}}_3) = 2$, where $\tilde{\mathbf{b}}_{1,2,3}$ are the reciprocal lattice vectors. The topological features of strong topological insulators (STI) are robust against the presence of time-reversal invariant perturbations such as disorder or lattice imperfections. It has been theoretically predicted [1, 4] and experimentally verified [2] that the surface of a STI has an odd number of Dirac cones whose positions are determined by the projection of \mathbf{M}_0 on to the surface Brillouin zone. The position and number of these cones depend on both the nature of the surface concerned and the integers $\nu_{1,2,3}$. For several compounds such as HgTe and Bi₂Se₃, specific surfaces with a single Dirac cone near the Γ point of the 2D Brillouin zone have been found [2, 5]. Such a Dirac cone is described by the Hamiltonian

$$H = \frac{d\mathbf{k}_x d\mathbf{k}_y}{(2)^2} \gamma^y (\mathbf{k}) (\sim v_F \sim \mathbf{k} \cdot \mathbf{I}) \cdot \mathbf{k}; \quad (1)$$

where γ^i denotes the Pauli (identity) matrices in spin space, $\gamma^y = (\sigma_y; \mathbb{I})^T$ is the annihilation operator for the Dirac spinor, v_F is the Fermi velocity, and μ is the chemical potential [6]. Recently, several novel features of these surface Dirac electrons such as the existence of Majorana fermions in the presence of a magnet-superconductor interface on the surface [6, 7, 8], generation of a time-reversal symmetric $p_x + ip_y$ superconducting state via proximity to a s-wave superconductor [6], anomalous magnetoresistance of ferromagnet-ferromagnet junctions [9] and novel spin textures with chiral properties [10] have been studied in detail.

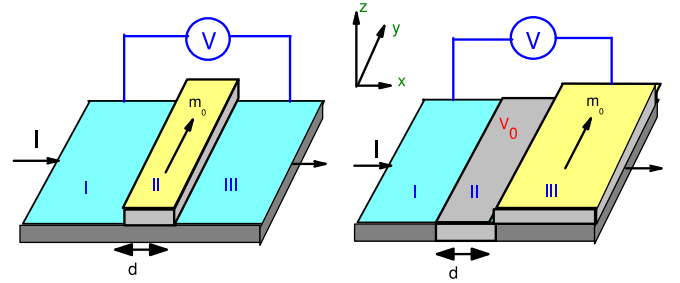


FIG. 1: Proposed experimental setups: a) Left panel: The ferromagnetic film extends over region II of width d providing an exchange field in this region. b) Right panel: The film extends over region III while the region II has a barrier characterized by a voltage V_0 . V and I denote the bias voltage and current across the junction respectively. See text for details.

In this letter, we study the transport properties of these surface Dirac fermions in two experimentally realizable situations shown in Fig. 1. The first study concerns their transport across a region with a width d with a proximity-induced exchange field J arising from the magnetization $\mathbf{m} = m_0 \hat{y}$ of a proximate ferromagnetic film as shown in the left panel of Fig. 1. We demonstrate that the tunneling conductance G of these Dirac fermions through such a junction can either be an oscillatory or a monotonically decaying function of the junction width d . One can interpolate between these two qualitatively different behaviors of G by changing m_0 (and thus J) by an applied in-plane magnetic field leading to the possible use of this junction as a magnetic switch. The second study concerns the transport properties of Dirac fermions across a barrier characterized by a width d and a potential V_0 in region II with a magnetic film proximate to region III as shown in the right panel of Fig. 1. We note that it is well known from the context of Dirac fermions in graphene [11] that such a junction,

in the absence of the induced magnetization, exhibits transmission resonances with maxima of transmission at $\epsilon V_0 d = \sim v_F = n$, where n is an integer. Here we show that beyond a critical strength of m_0 , the maxima of the transmission shifts to $\epsilon V_0 d = (n+1/2)$. Upon further increasing m_0 , one can reach a regime where the conductance across the junctions vanishes. We stress that the properties of Dirac fermions elucidated in both these studies are a consequence of their spinor structure in physical spin space, and thus have no analogs for either conventional Schrodinger electrons in 2D or Dirac electrons in graphene [12].

We begin with an analysis of the junction shown in the left panel of Fig. 1. The Dirac fermions in region I and III are described by the Hamiltonian in Eq. (1). Consequently, the wave functions of these fermions moving along x in these regions for a fixed transverse momentum k_y and energy can be written as

$$\psi_I = (1; e^i) e^{i(k_x x + k_y y)} = \frac{P}{2}; \quad (2)$$

where i takes values I and III, $\theta = \arcsin(\sim v_F k_y = j + \frac{1}{2})$ and $k_x(\theta) = \frac{[(\epsilon V_0 d)^2 - \sim v_F^2]^{1/2}}{\sim v_F}$. In region II, the presence of the ferromagnetic strip with a magnetization $m_0 = m_0 \hat{y}$ leads to the additional term $H_{\text{induced}} = \int dx dy J(x) (d-x)^y (\hat{x})_y (\hat{x})$, where $J = m_0$ is the exchange field due to the presence of the strip [9], and \hat{x} denotes the Heaviside step function. Note that H_{induced} may be thought as a vector potential term arising due to a fictitious magnetic field $B_f = (J = \epsilon v_F) [(\hat{x}) - (d-x)]\hat{z}$. This analogy shows that our choice of the in-plane magnetization along \hat{y} is completely general; all gauge invariant quantities such as transmission are independent of x -component of m_0 in the present geometry. For a given m_0 , the precise magnitude of J depends on several factors such as the exchange coupling of the Im and can be tuned, for soft ferromagnetic Im s, by an externally applied field [9]. The wave function for the Dirac fermions in region II moving along x in the presence of such an exchange field is given by

$$\psi_{II} = (1; e^i) e^{i(k_x^0 x + k_y y)} = \frac{P}{2}; \quad (3)$$

where $\theta = \arcsin(\sim v_F (k_y + M) = j + \frac{1}{2})$, $M = J(\sim v_F)$, and $k_x^0(\theta) = \frac{[(\epsilon V_0 d)^2 - \sim v_F^2]^{1/2}}{\sim v_F}$. Note that beyond a critical $M_c = 2j + \frac{1}{2}(\sim v_F)$ (and hence a critical $J_c = 2j + \frac{1}{2}$), k_x^0 becomes imaginary for all k_y leading to spatially decaying modes in region II.

Let us now consider an electron incident on region II from the left with a transverse momentum k_y and energy ϵ . Taking into account reflection and transmission processes at $x = 0$ and $x = d$, the wave function of the electron can be written as $\psi_I = \psi_I^+ + r \psi_I^-$, $\psi_{II} = p \psi_{II}^+ + q \psi_{II}^-$, and $\psi_{III} = t \psi_{III}^+$. Here r and t are the reflection and transmission amplitudes and p (q) denotes the amplitude of right (left) moving electrons in region II. Matching

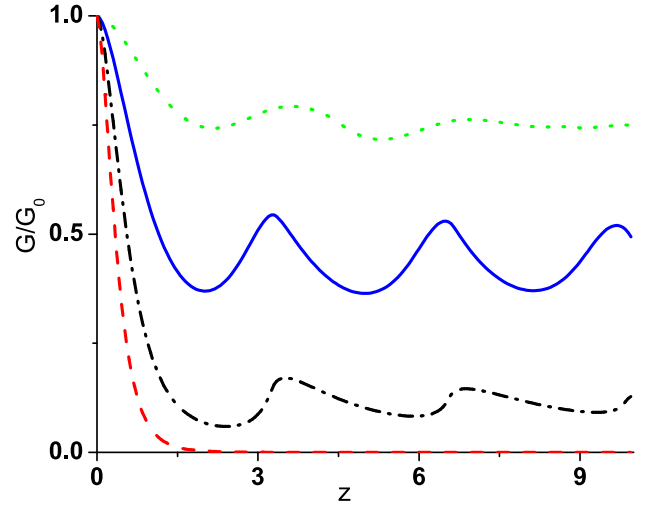


FIG. 2: Plot of tunneling conductance $G = G_0$ for a fixed V and d as a function of the effective width $z = d \epsilon V_0 + \frac{1}{2} \sim v_F$ for $\sim v_F M = \epsilon V_0 d + \frac{1}{2} \sim v_F$ (green dotted line), 0.7 (blue solid line), 1.3 (black dash-dotted line) and 2.1 (red dashed line). The value of the critical M_c is given by $\sim v_F M_c = \epsilon V_0 d + \frac{1}{2} \sim v_F = 2$. See text for details.

boundary conditions on ψ_I and ψ_{II} at $x = 0$ and ψ_{II} and ψ_{III} at $x = d$ leads to

$$\begin{aligned} 1 + r &= p + q; \quad e^i \psi_I = p e^i \psi_{II} + q e^i \psi_{III}; \\ t e^{i k_x d} &= p e^{i k_x^0 d} + q e^{i k_x^0 d}; \\ t e^{i(k_x d + \theta)} &= p e^{i(k_x^0 d + \theta)} + q e^{i(k_x^0 d + \theta)}; \end{aligned} \quad (4)$$

Solving for t from Eq. (4), one finally obtains the conductance $G = dI/dV = (G_0/2) \cos^2(\theta) d$. Here $G_0 = (\epsilon V_0) w e^2 = (\sim v_F^2) w$, $(\epsilon V_0) = \frac{1}{2} (\epsilon V_0 d + \frac{1}{2} \sim v_F)^2$ is the density of states (DOS) of the Dirac fermions and is a constant for $\epsilon V_0 d > \frac{1}{2} \sim v_F$, w is the sample width, and the transmission $T = \frac{G}{G_0}$ is given by

$$T = \cos^2(\theta) \cos^2(\theta) = [\cos^2(k_x^0 d) \cos^2(\theta) \cos^2(\theta) + \sin^2(k_x^0 d) (1 - \sin^2(\theta) \sin^2(\theta))] \quad (5)$$

Eq. (5) and the expression for G represent one of the main results of this work. We note that for a given d , T has an oscillatory (monotonically decaying) dependence on d provided k_x^0 is real (imaginary). Since k_x^0 depends, for a given d , on M , we find that one can switch from an oscillatory to a monotonically decaying d dependence of transmission in a given channel (labeled by k_y or equivalently θ) by turning on a magnetic field which controls m_0 and hence M . Also since $0 \leq \sin(\theta) \leq 1$, we find that beyond a critical $M = M_c$, the transmission in all channels exhibits a monotonically decaying dependence on d . Consequently, for a thick enough junction one can tune G at fixed V and d from a finite value to nearly zero by tuning M (i.e., m_0) through M_c . Thus such a junction may

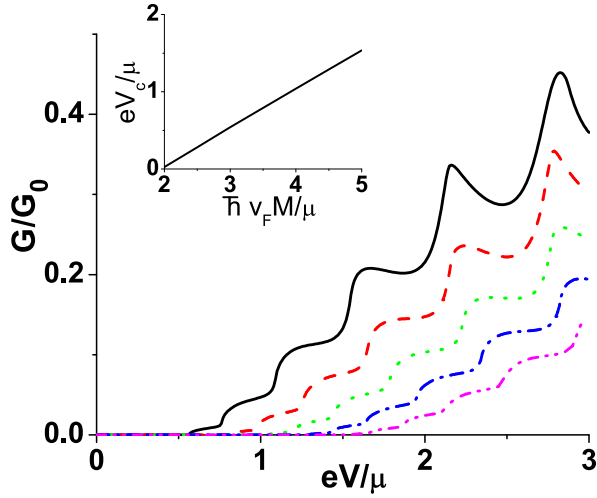


FIG. 3: Plot G/G_0 versus eV/μ for several representative values $\hbar v_F M/\mu$ ranging from 3 (left-most black solid curve) to 5 (right-most magenta dash-dotted line) in steps of 0.5. The effective junction width $z_0 = 5$ for all plots. The inset shows a plot of eV_c/μ versus $\hbar v_F M/\mu$. See text for details.

be used as a magnetic switch. These qualitatively different behaviors of the junction conductance G for M below and above M_c is demonstrated in Fig. 2 by plotting G as a function of effective barrier width $z = d[jV + \hbar v_F M]$ for several representative values of $\hbar v_F M = jV + \hbar v_F M_c$. Since T and hence G depends on M through the dimensionless parameter $\hbar v_F M = jV + \hbar v_F M_c$, this effect can also be observed by varying the applied voltage V for a fixed d , and M . In that case, for a reasonably large dimensionless barrier thickness $z_0 = d/\hbar v_F$, G/G_0 becomes finite only beyond a critical voltage $jV_c + \hbar v_F M_c = \hbar v_F M = 2$ as shown in Fig. 3 for several representative values of z_0 . This critical voltage V_c can be determined numerically by finding the lowest voltage for which G/G_0 exhibits a monotonic decay as a function of z_0 . The plot of eV_c/μ as a function of $\hbar v_F M/\mu$, shown in inset of Fig. 3, demonstrates the expected linear relationship between V_c and M . We note such a magnetic field or applied bias voltage dependence of the junction conductance necessitates that the Dirac electrons represents spinors in physical spin space and is therefore impossible to achieve in graphene [11].

Next, we analyze the junction shown in the right panel of Fig. 1 where the region III below a ferromagnetic film is separated from region I by a potential barrier in region II. Such a barrier can be applied by changing the chemical region in region II either by a gate voltage V_0 or via doping [5]. In the rest of this work, we will analyze the problem in the thin barrier limit for which $V_0 \ll 1$ and $d \ll 0$, keeping the dimensionless barrier strength $\tilde{V} = eV_0 d/(\hbar v_F)$ finite. The wave function of the Dirac fermions moving along x with a fixed momentum k_y

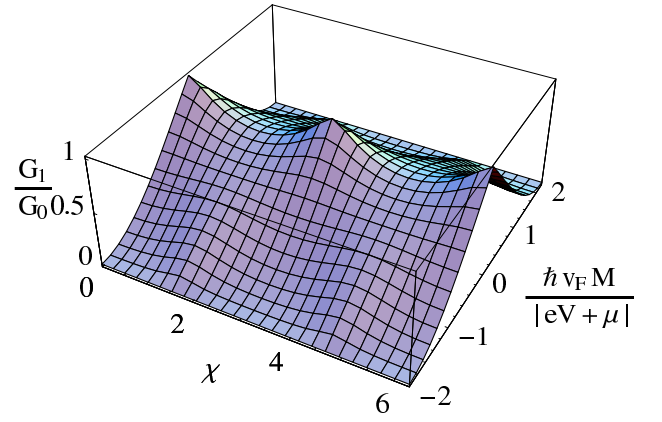


FIG. 4: Plot of tunneling conductance $G_1 = G_0$ versus the effective barrier strength χ and $\hbar v_F M$ for fixed applied voltage V and chemical potential μ . G_1 vanishes for $M < M_c = 2jV + \hbar v_F M_c$.

and energy in this region is given by

$$\psi_{\text{III}}^0 = (1; e^{i\theta}) e^{i(k_x^0 x + k_y y)} = \frac{P}{2}; \quad (6)$$

where $\theta = \arcsin(\hbar v_F k_y / j + eV_0 + \hbar v_F M_c)$ and $k_x^0(\theta) = \sqrt{[(j + eV_0 + \hbar v_F M_c) - \hbar v_F]^2 - k_y^2}$. The wave functions in region I and III are given by Eqs. (2) and (3) respectively: $\psi_{\text{I}}^0 = \psi_{\text{I}}$ and $\psi_{\text{III}}^0 = \psi_{\text{II}}$. Note that one can have a propagating solution in region III only if $M > M_c$.

The transmission problem for such a junction can be solved by an procedure similar to the one outlined above for the magnetic strip problem. For an electron approaching the barrier region from the left, we write down forms of the wave function in the three regions I, II and III: $\psi_{\text{I}}^0 = \psi_{\text{I}}^+ + r_1 \psi_{\text{I}}^-$, $\psi_{\text{II}}^0 = p_1 \psi_{\text{II}}^+ + q_1 \psi_{\text{II}}^-$, and $\psi_{\text{III}}^0 = t_1 \psi_{\text{III}}^+$. As outlined earlier, one can then match boundary conditions at $x = 0$ and $x = d$, and obtain the transmission coefficient $T_1 = |t_1|^2 / |k_x^0| = k_x$ as

$$T_1 = \frac{2 \cos(\theta) \cos(\theta')}{\cos^2(\theta) + \cos^2(\theta') + \cos(\theta + \theta')g}; \quad (7)$$

Note that in the absence of the ferromagnetic film over region III, $\theta = 0$, and $T_1 \rightarrow T_1^0 = \cos^2(\theta') = [1 - \cos^2(\theta') \sin^2(\theta')]$. The expression for T_1^0 , reproduced here for the special case of $M = 0$, is well known from analogous studies in the context of graphene, and it exhibits both Klein paradox ($T_1^0 = 1$ for $\theta' = 0$) and transmission resonance ($T_1^0 = 1$ for $\theta' = n\pi$) [12]. When $M \neq 0$, we find that the transmission for normal incidence ($k_y = 0$) does become independent of the barrier strength, but its magnitude deviates from unity: $T_1^{\text{normal}} = \frac{2}{1 + (\hbar v_F M_c)^2} = \frac{2}{1 + (\hbar v_F M_c)^2}$. The value of T_1^{normal} decreases monotonically from 1 for $M_c = 0$ to 0 for $M_c = \hbar v_F$ and can thus be tuned by changing M (or V) for a fixed V (or M) and μ .

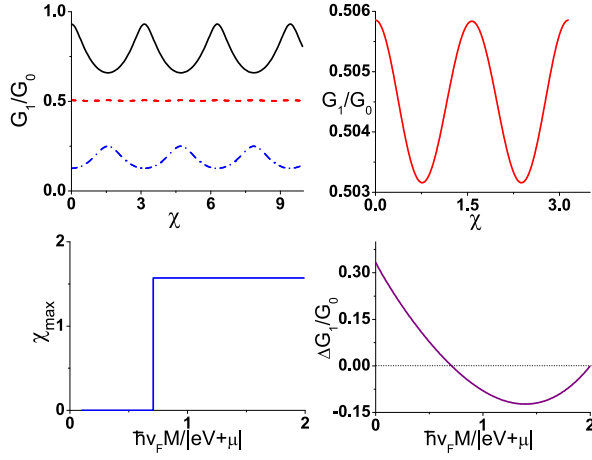


FIG. 5: Top left panel: Plot of $G_1=G_0$ versus χ for $\sim v_F M = jV + j = 0.1$ (black solid line), 0.7075 (red dashed line), and 1.4 (blue dash-dotted line) for fixed V and j . Top right panel: Plot of $G_1=G_0$ versus χ at $M = M_c$ showing the period halving. Bottom left panel: Plot of χ_{\max} versus $\sim v_F M = jV + j$ showing the shift of conductance maxima. Bottom right panel: Plot of $\Delta G_1=G_0$ versus $\sim v_F M = jV + j$ which crosses 0 for $M < M_c$ at $M = M_c$. The dotted line is a guide to the eye.

The conductance of such a junction is given by $G_1 = (G_0=2)^{-1} T_1 \cos(\chi) d$, where $\chi_{1,2}$ are determined from the solution of $\cos(\chi) = 0$ for a given M (Eq. (3)). A plot of G_1 as a function of $\sim v_F M = jV + j$ and χ (for a fixed eV and j) is shown in Fig. 4. We find that the amplitude of G_1 decreases monotonically as a function of M reaching 0 at $M = M_c$ beyond which there are no propagating modes in region III. Also, as we increase M , the conductance maxima shifts from $\chi = n$ to $\chi = (n+1=2)$ beyond a fixed value of M (V)' $q jV + j (\sim v_F)$ as shown in top left panel of Fig. 5. Numerically, we find $c_0 = 0.7075$. At $M = M_c$, $G_1(\chi = n) = G_1(\chi = (n+1=2))$, leading to a period halving of $G_1(\chi)$ from π to 2π . This is shown in top right panel of Fig. 5 where $G_1(M = M_c)$ is plotted as a function of χ . We note that near M_c , the amplitude of oscillation of G_1 as a function of χ becomes very small so that G_1 is almost independent of χ . In the bottom left panel of Fig. 5, we plot χ_{\max} (the value of χ at which the first conductance maxima occurs) as a function of $\sim v_F M = jV + j$ which clearly demonstrates the shift. This is further highlighted by plotting $G_1 = G_1(\chi = 0) - G_1(\chi = 2\pi)$ as a function of $\sim v_F M = jV + j$ in the bottom right panel of Fig. 5. For $M < M_c$, G_1 crosses zero at $M = M_c$ indicating the position of the above-mentioned period halving. Thus we conclude that the position of the conductance maxima depends crucially on $\sim v_F M = jV + j$ and can be tuned by changing either M or V .

The experimental verification of our results would involve preparation of junctions by depositing ferromagnetic films on the surface of a topological insulator. For

the geometry shown in the left panel of Fig. 1, we propose measurement of G as a function of m_0 whose magnitude and direction can be tuned by an externally applied in-plane magnetic field for soft ferromagnetic films [9]. We predict that depending on m_0 , G should demonstrate either a monotonically decreasing or an oscillatory behavior as a function of d . Another, probably more experimentally convenient, way to realize this effect would be to measure V_c of a junction of width d for several M and confirm that V_c varies linearly with M with a slope of $\sim v_F = (2e)$, provided χ and d remain fixed. For the geometry depicted in the right panel of Fig. 1, one would, in addition, need to create a barrier by tuning the chemical potential of an intermediate thin region of the sample as done earlier for graphene [11]. Here we propose measurement of G_1 as a function of V_0 (or equivalently χ) for several representative values of m_0 and a fixed V . We predict that the maxima of the tunneling conductance would shift from $\chi = n$ to $\chi = (n+1=2)$ beyond a critical m_0 for a fixed V , or equivalently, below a critical V , for a fixed m_0 .

In conclusion, we have studied the transport of Dirac fermions on the surface of a topological insulator in the presence of proximate ferromagnetic films in two experimentally realizable geometries. Our study unravels novel features of the junction conductances which have no analog in either graphene or 2D Schrodinger electrons and can be verified in realistic experimental setups.

- [1] B. A. Bernevig, T. L. Hughes, and S. C. Zhang, *Science* 314, 1757 (2006).
- [2] M. Koenig et al., *Science* 318, 766 (2007); D. Hsieh et al., *Nature* 452, 970 (2008);
- [3] C. L. Kane and E. J. Mele, *Phys. Rev. Lett.* 95, 226801 (1995); *ibid*, *Phys. Rev. Lett.* 95, 146802 (2006).
- [4] L. Fu, C. L. Kane, and E. J. Mele, *Phys. Rev. Lett.* 98, 106803 (2007); R. Roy, *arXiv:cond-mat/0607531* (unpublished); J. E. Moore and L. Balents, *Phys. Rev. B* 75, 121306 (2007).
- [5] Y. Xia et al., *Nature Phys.* 5, 398 (2009); *ibid*, *arXiv:0907.3089* (unpublished).
- [6] L. Fu and C. L. Kane, *Phys. Rev. Lett.* 100, 096407 (2008).
- [7] A. R. Akhmerov, J. Nilsson, and C. W. J. Beenakker, *Phys. Rev. Lett.* 102, 216404 (2009).
- [8] Y. Tanaka, T. Yokoyama, and N. Nagaosa, *arXiv:0907.2088* (unpublished).
- [9] T. Yokoyama, Y. Tanaka, and N. Nagaosa, *arXiv:0907.2810* (unpublished).
- [10] D. Hsieh et al., *Science* 323 919 (2009); D. Hsieh et al., *arXiv:0904.1260* (unpublished).
- [11] A. Castro Neto et al., *Rev. Mod. Phys.* 81, 109 (2009); C. W. J. Beenakker, *Rev. Mod. Phys.* 80, 1337 (2008); A. K. Geim, *Science* 324, 1530 (2009).
- [12] M. I. Katsnelson, K. S. Novoselov, and A. K. Geim, *Nature Phys.* 2, 620 (2006); C. W. J. Beenakker, *Phys. Rev. Lett.* 97, 067007 (2006); S. Bhattacharjee and K. Sengupta, *Phys. Rev. Lett.* 97, 217001 (2006).